Recombinant production of human ICAM-1 chimeras by single step on column refolding and purification.

David Núñez[1,2], María Pilar Domingo[1,2], Diego Sánchez-Martínez[2,3], Vicente Cebolla[1], Arthur Chiou[4], Adrián Velázquez-Campoy[3,5,6], Julián Pardo[2,3,6,7‡] and Eva Mª Gálvez[1,2*‡]

[1] Instituto de Carboquímica ICB-CSIC, Zaragoza, Spain

[2] Immune Effector Cells Group, Aragón Health Research Institute (IIS Aragón), Biomedical Research Centre of Aragón (CIBA)

[3] Dpt. Biochemistry and Molecular and Cell Biology, Fac. Ciencias, University of Zaragoza, Zaragoza, Spain

[4] Institute of Biophotonics, National Yang-Ming University, Taipei, Taiwan

[5] Institute of Biocomputation and Physics of Complex Systems (BIFI), Unidad Asociada IQFR-CSIC-BIFI, Universidad de Zaragoza, Zaragoza, Spain.

[6] Aragón I+D Foundation (ARAID), Government of Aragon, Zaragoza, Spain

[7] Nanoscience Institute of Aragon (INA). Aragón I+D Foundation (ARAID). University of Zaragoza, Zaragoza, Spain

* Corresponding author. Tel.: +34-976733977. E-mail address: eva@icb.csic.es (E. Galvez).

‡ These authors contributed equally to this work.

Keywords: Adhesion molecules, on-column refolding, LFA-1

Summary

The interaction of the adhesion molecule of the immunoglobulin family Intercellular Adhesion Molecule 1 (ICAM-1) with its ligands such the integrins LFA-1 and Mac-1 is crucial for the regulation of several physiological and pathophysiological processes like cell mediated-elimination of tumor or virus infected cells, cancer metastasis or inflammatory autoimmune processes. Thus, production of milligrams of protein is required to perform structural and functional studies as well as design novel approaches to find out new inhibitors of ICAM-1/LFA-1 interaction. Here we report on the production of a recombinant human ICAM-1 chimera comprising the first two extracellular domains of ICAM-1 linked to the Fc fraction of a human IgG1. To this aim we have used a cost-effective method based on the expression of a His-tagged protein in *E. coli* followed by a single step of refolding and purification on immobilized metal affinity columns. This method is able to produce 3mg/liter of bacterial culture in just 72 hours with purity greater than 95%. The identity and the native structure of refolded human ICAM-1 chimera were confirmed by biochemical and biophysical studies including SDS-electrophoresis, immunoblot, circular dichroism, isothermal titration calorimetry and fluorescence spectroscopy. Native folding and functional activity of the chimera were further confirmed by different cell biology studies, including B cell adhesion, T cell binding and inhibition of NK cell function. These studies indicate a high biological activity of the protein since it induces a 200-fold increase/mg of protein in B cell adhesion and the Inhibitory Dose 50 to block cell-mediated cytotoxicity is 10 pg/effector cell. These analyses show that our protocol is able to produce a recombinant human ICAM-1 chimera fully active and useful to analyse the biological processes in which ICAM-1/LFA-1 interaction is critically involved.

Introduction

The intercellular adhesion molecule 1 (ICAM-1) is a membrane glycoprotein, member of the immunoglobulin superfamily (IgSF) and responsible for mediating cell-cell and cell-extracellular matrix interactions [1-3]. In addition, ICAM-1 is the receptor for different human viruses like rhinovirus [4] and coxsackievirus A21 as well as for the malarial parasite *Plasmodium falciparum* [5-7]. ICAM-1 is formed by 5 extracellular immunoglobulin domains, a hydrophobic transmembrane domain and a short cytoplasmic tail and expressed by several cell types including endothelial and epithelial cells and most types of leukocytes including B and T lymphocytes, NK cells and monocytes [3] [1]. Although the protein is heavily glycosylated, glycosylation does not affect the interaction between ICAM-1 and the integrin LFA-1 [8, 9]. This interaction occurs between domain 1 of ICAM-1 [10] and a metal ion-dependent adhesion site (MIDAS) motif located in the integrin α subunit I domain [11, 12]. Domain 1 of ICAM-1 also contains the interaction site with human rhinovirus [13] and *Plasmodium falciparum* [5] as well as for the extracellular matrix protein fibrinogen [14]. The integrin Mac1 binds to domain 3 of ICAM-1 [8]. ICAM-1 is expressed as a dimer in the plasma membrane of cells and this form binds more efficiently to LFA-1 than monomeric ICAM-1 [15, 16]. However, the crystal structure of dimeric ICAM-1 suggests that the dimer is not required for binding of LFA-1 and rhinovirus [17], which occurs by a single molecule of ICAM-1 [18]. In fact monomeric recombinant ICAM-1 prevents development of insulitis during autoimmune diabetes [19]. Finally, it has been recently reported that the equilibrium between monomeric and dimeric state regulates the binding to LFA-1 [20].

The interaction of ICAM-1 with LFA-1 regulates several physiological and pathophysiological processes related with lymphocyte extravasation to inflammatory sites and selective entry into lymphoid organs (lymphocyte homing) [3, 21, 22]. In addition, this interaction is critically involved in cell-cell adhesion during antigen presentation and during the recognition and elimination of tumor or virus-infected cells [23]. Apart from its beneficial effect in the elimination of tumor cells and pathogens, ICAM-1/LFA-1 interaction is also involved in diverse pathologies involving inflammation and/or cellular extravasation [24]. It has been shown that specific tumour cells use this interaction to disseminate and spread to other tissues or organs [25-27] and that ICAM-1 expression contributes to drug resistance in multiple myeloma [28]. In

addition, lymphocyte extravasation and accumulation in diverse tissues mediated by LFA-1 is associated with inflammatory diseases like Rheumathoid Arthritis [29], Atherosclerosis [30] and Inflammatory Bowel Disease [31, 32] among others. Altogether, these findings suggest that targeting ICAM-1/LFA-1 interaction may help to inhibit tumor spreading [33] or to treat inflammatory disorders [33, 34] [35].

Several chromatographic approaches have been previously developed in order to purify and refold recombinant mammal proteins produced in bacterial systems. Among them Immobilised Metal Affinity Chromatography (IMAC) has been proved to be especially useful to purify proteins genetically modified to contain an amino- or carboxy-terminal polyhistidine sequences (His-Tag). This type of affinity chromatography is based on the ability of divalent cations like Cu^{2+}, Co^{2+} or Ni^{2+} to bind imidazole groups from histidine residues [36, 37]. In order to bind efficiently the protein multiple histidine groups must located in close proximity. Very few proteins fulfil this prerequisite and, thus, this type of chromatography simplifies the whole purification process. This is especially true if purification is performed under denatured conditions, since the possibility of histidine groups closely located due to the native three-dimensional structure is eliminated.

One of the main problems of producing mammal proteins in prokaryotic systems is that proteins are usually expressed as a type of insoluble material known as inclusion bodies. In order to circumvent this problem and get functional proteins in native form *in vitro* refolding must be performed.

Among the different protocols used to refold proteins *in vitro*, [38], it seems that addition of detergents to refolding buffer helps to minimise the formation of aggregates and improves the refold efficiency [39]. A singular advance to avoid the use of large amounts of buffers and time invested in refolding by dilution was the introduction of the on column refolding [40]. Most types of chromatographic methods have been used to refold proteins on columns including size exclusion chromatography [41, 42] immobilization on gel matrices [43], hydrophobic interaction chromatography [44], affinity chromatography [45], immobilized liposome chromatography [46] and IMAC [40, 47-50].

Generation of purified active forms of ICAM-1 is very important to study the above-mentioned functions. Specially, the availability of large amounts of active ICAM-1 is

crucial to design efficient and specific approaches to find new inhibitors of ICAM-1/LFA-1 interaction.

To this aim we have established a simple and fast protocol to generate large quantities of active ICAM-1 chimera in *Escherichia coli* by reducing the timing and reagents and, thus, improving the efficiency of the process. His-tagged protein is expressed in bacteria as inclusion bodies and refolded and purified in a single step by using Immobilised Metal Affinity Chromatography (IMAC). Our method shows a reduction in total process time of up to 500% and decreases the cost of up to 150% in comparison with refolding by dilution, the most common protocol to purify ICAM-1 in *E. coli* [9]. The purity of ICAM-1 is greater than 95% and the yield is 3 mg/liter of bacterial culture. Moreover, the activity of ICAM-1 has been proven by using biochemical, biophysical and cell biology models.

Materials and methods

Plasmids and bacterial strains

Two synthetic cDNAs corresponding to the first two domains (D_1D_2) of human ICAM1 or D_1D_2 linked to human IgG1 Fc region cloned into pET28a(+) plasmid at NdeI/EcoR1 sites (Figure 1) were purchased from GenScript (Piscataway, NJ, USA). Plasmids were transformed into chemically competent BL21 *Escherichia coli* strain BL21 CodonPlus (Novagen) for high-level protein expression. The proteins expressed by using these constructs contain a 6 histidine-tag at the N-terminal site.

Expression and Purification of D_1D_2Fc and D_1D_2

Bacterial cultures containing pET28a-D_1D_2Fc or pET28a-D_1D_2 were grown at 37ºC until the optical density (OD) at 600 nm reached 0.6-0.8. Subsequently, protein expression was induced by adding isopropyl-beta-D-1-galactopyranoside (IPTG) to a final concentration of 1mM for 3 h at 37ºC. After protein induction cells were recovered by centrifugation at 17,700 g for 8 min at 4ºC. Proteins were solubilised from inclusion bodies by resuspending the cell pellets in 6 M guanidine hydrochloride (GdmCl) at room temperature with gently shaking overnight. Subsequently, cell suspension was centrifuged at 48,400 g for 30 min at 4ºC to pellet cellular debris. Supernatants containing the soluble proteins were then recovered and incubated for 1 hour at room temperature with Ni-NTA resin (Qiagen, Hilden, Germany) to allow the polyhistidine tag to bind to the resin. After centrifugation at 157 g for 2 min, most of the supernatant was carefully removed and then resin was resuspended in the remaining supernatant, transferred to a gravity-flow column and allowed to settle.

On-column renaturation and purification was performed by several changes of buffers following a modified protocol based on that described by Oganesyan [47]. First, the column was washed using the denaturing buffer containing 20mM imidazole to remove non-specifically-bound contaminants and mercaptoethanol 10mM to reduce disulfide bonds. Then, renaturation was carried on using buffer A (20mM Tris-HCl pH 8.0, 0.1M NaCl). In the first step, the column was washed with 10-column volumes (CV) of buffer A containing 0.1% Triton X-100 and mercaptoethanol 10mM. Next, resin was washed with 10 CV of buffer A containing 5mM Methyl-β-cyclodextrin (Sigma, St.Louis, Missouri, USA) to remove detergent from the protein-detergent complex and to allow the protein to refold. The last wash before elution was performed with 20mM Tris-HCl pH 8.0, 0.5M NaCl to remove remaining impurities and Methyl-β-cyclodextrin. All

steps were performed in the presence of a cocktail of protease inhibitors (Roche, Basel, Switzerland). Refolded protein was eluted with buffer A containing 1 M imidazole and protein concentration was measured using a spectrophotometer (NanoView, Healthcare, Waukesha, WI, USA). Fractions containing the highest levels of protein were passed through a desalting column (PD-10 Desalting Columns, GE Healthcare, Waukesha, WI, USA) following manufacturer's instructions and the protein was recovered in phosphate buffered saline (PBS). Protein concentration was adjusted to 500µg/ml by ultrafiltration using 10,000 MWCO Centrifugal Filter Units (Amicon, Millipore, Billerica, MA, USA) and stored at -20ºC. The level of protein expression after IPTG induction and the quality of purified proteins was evaluated by sodium dodecyl sulfate polyacrylamide gel electrophoresis (SDS–PAGE) under reducing conditions and staining with Coomassie Blue.

Western blot analysis

Purified D_1D_2Fc and D_1D_2 was analysed by western blotting under reducing conditions by using a mouse mAb against human CD54/ICAM1 (clone 28/CD54; BD bioscience, San Jose, CA, USA; dilution 1:1000) or a mouse mAb against HisTag (Novagen, Madison, WI, USA; dilution 1:1000). Then, the blot was stained with peroxidase-conjugated secondary antibodies, rabbit anti-mouse (Amersham, Piscataway, NJ, USA; dilution 1:10000). Subsequently, a peroxidase substrate for enhanced chemiluminescence (ECL) from Pierce (Rockford, IL, USA) was used for detection.

Circular dichroism spectroscopy

Secondary structure of proteins was examined using circular dichroism (CD) in a Chirascan spectropolarimeter (Applied Photophysics). Spectra were recorded in the far ultraviolet region (200nm-250nm) with a protein concentration of 6µM in PBS (Phosphate buffered saline) and a scan rate of 1 nm/s. The temperature was controlled by a Peltier controller. It was employed a quartz cuvette 0.1cm path length.

Fluorescence Spectroscopy

Protein samples were characterized by fluorescence spectroscopy using a Cary Eclipse spectrofluorometer (Varian, Palo Alto, CA, USA) thermostated by a Peltier temperature control unit, employing either the fluorescence emission from the internal tryptophan residues or from the ANS (8-anilino-1-naphthalenesulfonic acid) extrinsic probe. When

convenient, the fluorescence intensity at a certain wavelength, I_λ, or the average energy of the spectrum:

$$\text{Average Energy} = \frac{\sum_n I_i e^{i}}{\sum_n I_i}$$

was considered as the reporting signal. Protein samples were excited at 290 nm and 390 nm when tryptophan and ANS spectra were recorded, respectively, with a slit width of 5 nm.

Thermal unfolding assays were conducted in order to assess the structural stability of the proteins. An unfolding model considering an intermediate partially folded state was employed:

$$S(T) = F_N(T)I_N(T) + F_I(T)I_I(T) + F_U(T)I_U(T)$$

where T is the absolute temperature; S(T) is either the fluorescence intensity at a certain wavelength or the average energy of the spectrum; I_N, I_I and I_U are the intrinsic contributions to the fluorescence of each conformational state, that are assumed to exhibit a linear dependency with the temperature:

$$I_X(T) = a_X + b_X T$$

and $F_N(T)$, $F_I(T)$ and $F_U(T)$ are the fraction population of each conformational state (native, intermediate and unfolded) and can be expressed in terms of the equilibrium constants associated with each conformational transition, $K_1(T)$ and $K_2(T)$:

$$F_N(T) = \frac{1}{1 + K_1(T) + K_1(T)K_2(T)}$$

$$F_N(T) = \frac{K_1(T)}{1 + K_1(T) + K_1(T)K_2(T)}$$

$$F_N(T) = \frac{K_1(T)K_2(T)}{1 + K_1(T) + K_1(T)K_2(T)}$$

The equilibrium constants are also temperature dependent:

$$K_i(T) = \exp\left[\frac{1}{RT}\left(H_i - \frac{T}{T_{mi}}\right) - C_{Pi}\left(T - T_{mi} - T\ln\frac{T}{T_{mi}}\right)\right]$$

where R is the ideal gas constant, T_{mi} is the unfolding (or mid-transition) temperature, ΔH_i is the unfolding enthalpy, and ΔC_{Pi} is the unfolding heat capacity for each transition i. Non-linear square regression data analysis implemented in Origin (OriginLab) provides the unfolding parameters (T_{mi}, ΔH_i, and ΔC_{Pi}) for both proteins, D_1D_2Fc and D_1D_2.

Isothermal titration calorimetry

The ability of D_1D_2Fc to interact with a peptide derived from its natural ligand LFA-1 was analysed by isothermal titration calorimetry (ITC) on a VP-ITC calorimeter (MicroCal) at 25 °C. The peptide sequence was DSGNIDAAKD corresponding to aminoacids 244-253 from LFA-1 [51]. 2.2 ml of a 12 μM solution of D_1D_2Fc and 0.6 ml of a 150 mM solution of peptide were prepared in PBS and degassed with a vacuum pump for 10 min. Protein solution was carefully injected into the cell previously washed with PBS. Each assay consisted of a series of 28 injections of peptide solution of 10 ul each (with a 4-μl first onjection) at 400 s intervals under constant stirring (459 rpm). The thermal power required to keep the cell at a constant temperature is measured, so that it provides the heat associated with each ligand injection after integrating the signal over time. The thermodynamic parameters of protein-peptide interactions (affinity, enthalpy and entropy changes) as well as the stoichiometry were estimated by using nonlinear regression analysis. Data were analyzed using the software developed and implemented in Origin 7.0 (OriginLab).

Cell Adhesion assay

The ability of ICAM1 chimera (D_1D_2Fc) to induce cell adhesion of non-adherent cells expressing LFA-1 was analysed by using the EBV transformed human B lymphoblastoid cell line R69, a generous gift from José A. López de Castro [52]. Adhesion assay was performed in flat bottom 96-well plates in which different amounts of ICAM-1 chimera or human IgG1 (Fc control) had been previously immobilized for 18h at 4ºC. R69 human cells were washed twice in DMEM medium supplemented with 10% fetal bovine serum, 2 mM L-glutamine and antibiotics (penicillin 100 U/ml, streptomycin 100 μg/ml) and resuspended at a final concentration of 10^6 cells/ml. Then, LFA-1 expression was induced by incubating cells with 10 ng/ml PMA for 2 hours at 37°C [53]. Subsequently, $1x10^5$ cells were added to each well and incubated at 37°C for

4 hours. To quantify the number of adherent cells a modification of the MTT colorimetric test designed by Mosmann [54] was used.

Flow cytometry (FACS)

The ability of D_1D_2Fc to quantify the expression of LFA-1 on cells was analysed by flow cytometry in the human T leukemia cell line Jurkat (clon E6-1, ATCC). Jurkat cells were incubated with different concentrations of D_1D_2Fc or human IgG1 control at 4°C for 30 min, washed twice with FACS buffer (PBS, 5% FCS, 0,1% NaN_3) and then incubated with PE-conjugated goat anti-human IgG (Fcγ fragment specific; Jackson ImmunoResearch). After a washing step with FACS buffer, cells were analysed by FACS using a FACSCalibur with CellQuest Pro software (BD).

Cytotoxicity assay

The effect of D_1D_2Fc and D_1D_2 on ICAM-1/LFA-1 dependent cell-cell contact was analysed by performing a cell cytotoxicity assay using human primary NK cells and the NK-cell sensitive human leukemia K562. Primary human NK cells were generated by culturing human peripheral blood mononuclear cells (PBMCs) with mitomycin C inactivated R69 cells for 5 days as previously described [55]. Then, NK cell fraction was enriched by MACS using anti-CD56 antibodies as previously described [56]. Cell cytotoxicity induced by NK cells on K562 was analyzed by flow cytometry as previously described [56]. Briefly, NK cells were preincubated with medium alone or in the presence of different amounts of D_1D_2Fc , D_1D_2 or human IgG1 control for 15 min at 37ºC. Then, they were added to K562 cells at different e:t cell ratio for 4h at 37ºC, 5% CO2. Subsequently, phosphatidylserine exposure and AAD uptake were analyzed by FACS using the annexin-V/AAD kit from BD Pharmingen.

Results and discussion

Expression of recombinant proteins

First we have analysed that *E. coli* BL21-Codon plus cells transformed with pET28a-D_1D_2Fc or pET28a-D_1D_2 overexpressed the respective proteins after induction with IPTG. As shown in Figure 2A, the expression of two proteins was clearly increased after 2 and 3 hours of induction. The approximate MW of these proteins was 50 kDa (lanes 2 and 3) and 25 kDa (lanes 5 and 6), which matched well with the theoretical MWs of D_1D_2Fc and D_1D_2, respectively. In contrast, non-induced cells did not express the proteins (lanes 1 and 4). The highest level of expression was found at 3 hours and longer induction times (4 and 24h) did not increase that level. Thus, we chose this time-point in the subsequent experiments.

Purification of recombinant proteins

Ni-NTA affinity chromatography was applied for the purification of D_1D_2 and D_1D_2Fc poly-histidine tagged proteins. Poly-histidine tags form high affinity complexes with immobilized divalent metal ions (such as Ni^{2+} or Co^{2+}), even in the presence of high concentrations of chaotropic agents (e.g., urea or GdmCl), thereby allowing isolation of tagged protein from a crude cellular extract [36, 37, 57]. In addition, these properties allow to refold denatured proteins by changing the buffer composition flowing through the column [40, 47-50]. Most of D_1D_2Fc and D_1D_2 exist in the bacterial cells in the form of inclusion bodies that were solubilized by resuspending bacterial pellets in 6M GdmCl. Soluble proteins were incubated with the Ni-NTA resin slurry to allow binding of the poly-histidine-tagged proteins and folded as indicated in methodological section. As shown in Figure 2B, non-bound proteins were washed out during the first two steps of purification (lanes 3 and 4). These fractions also contained some D_1D_2Fc protein, although at very low levels. Unbound proteins were not detected anymore in fractions corresponding to the folding steps (lanes 5 and 6). After folding the bound proteins, they were eluted by using imidazole. Most of D_1D_2Fc protein eluted in the early fractions (Figure 2B, lanes 8-12) which contained a small amount of proteins of lower MW, suggesting that either contaminating proteins co-eluated with D_1D_2Fc or some protein degradation ocurred during the purification process. In order to confirm the identity of the purified protein and of the low MW forms, we performed immunoblot using mAbs specific for ICAM-1 (Figure 2C, lane 1) or for the poly-histidine tag

(Figure 2C, lane 2). As shown in the blots a single band corresponding to D_1D_2Fc was detected by using anti-ICAM-1 mAb confirming the identity of the purified protein. In contrast, several bands were detected with the anti-HisTag antibody. The pattern of bands detected by this mAb matched those observed by Coomassie Blue staining (Figure 2B), confirming that the low MW proteins contains a poly-histidine tag and, thus, correspond to short forms of our fusion protein. Since poly-histidine tag is placed at the N-terminal site, this result indicates that degradation of the protein occurs at the C-terminal site where the Fc fraction is located. Moreover, it suggests that the epitope recognised by the anti-ICAM-1 mAb is missed in the degraded proteins. Anyway, the level of degradation is minimal since the intensity of the 50 KDa band corresponding to D_1D_2Fc was much stronger than that of the lower bands.

Similar results were found when D_1D_2 protein was purified (Figure 2D and 2E). However, no degradation products were observed in the purified fraction, confirming that the residual degradation of the D_1D_2Fc chimera occurred by the Fc fraction. This result is not surprising since it is known that Fc regions are especially susceptible to the action of specific proteases like pepsin-like proteases. However, this effect has been minimised by including general protease inhibitors during the purification process.

Altogether, the results indicate that the purified protein corresponds to the recombinant ICAM-1 D_1D_2Fc chimera and degradation is hardly observed. The yield obtained by using this protocol is around 3 mg per liter of bacterial culture and the entire process took just 72 hours from bacterial cultures to purified protein. Of note, the purification of other recombinant proteins using redolding by dilution takes about 14 days in our laboratory.

Circular dichroism

Next we have analysed by circular dichroism (CD) whether purified ICAM-1 D_1D_2Fc chimera is properly folded and presents the expected secondary structure. ICAM-1 belongs to the IgSF and each of its domains presents a typical Ig-like structure characterised by the presence of β-sheets [58]. Dichroism spectra in the far ultraviolet region are primarily due to the amide bonds linking the amino acid residues. The asymmetry of these chromophores is due to the spatial arrangement of the main chain of the protein, thus, the circular dichroism signals can be interpreted in terms of the content of secondary structure present, i.e. the percentage of residues found in some structural conformation (α helix, β sheets, turns and other structural types).

As shown in Figure 3A the CD spectrum of D_1D_2Fc shows a single broad negative ellipticity centered at approximately 205 nm. This result indicates that the protein predominatly contains β sheets or turns as secondary structures and, thus, that the folding protocol renders a protein with the expected secondary structure.

Fluorescence spectroscopy

Both D_1D_2Fc and D_1D_2 show a fluorescence spectrum with two maxima around 330 nm and 375 nm, in agreement with these two proteins containing several tryptophan residues (Figure 3B, i).

In order to test the structural integrity of the proteins, fluorescence thermal denaturations were performed (Figures 3B, ii-vi). Unfolding parameters for D_1D_2Fc following the thermal denaturation either by intrinsic tryptophan fluorescence or extrinsic ANS fluorescence provided similar results (Figures 3B, ii and iv, Table 1). However, for D_1D_2 only ANS fluorescence data showed a clear unfolding curve (Figure 3B, vi). Two transitions can be clearly observed for the unfolding behavior of D_1D_2Fc, whereas for D_1D_2 was not so evident. However, analysis of D_1D_2 unfolding employing a model considering a single transition provided illogical results (e.g. negative unfolding enthalpy, which is impossible for a temperature-driven process). Using the average energy of the spectrum presents two advantages: 1) signal is concentration-independent; and 2) global changes in the spectrum are taken into account, that could be overlooked when just paying attention to a certain wavelength. Because both proteins, D_1D_2Fc and D_1D_2, contain several tryptophan residues, interpretation of the results obtained when the intrinsic tryptophan fluorescence was employed as a reporter signal was somewhat difficult.

According to the data analysis, D_1D_2Fc showed two transitions with T_m's at 40°C and 70°C, and unfolding enthalpies of 20 and 50 kcal/mol, respectively. Deletion of the Fc domain leads to a slight stabilization of the less stable region and a destabilization of the more stable region (Table 1).

Isothermal titration calorimetry

CD and thermal denaturation data indicate that ICAM-1 chimera presents a proper secondary and tertiary structure folding. However, this does not mean that the protein is functionally active and able to recognise its natural ligands. To test D_1D_2Fc activity we

have analysed the interaction of this protein with a peptide derived from its natural ligand LFA-1 (DSGNIDAAKD) by isothermal titration calorimetry.

As shown in Figure 4 this peptide presents a high affinity for D_1D_2Fc (dissociation constant K_d of 0.090 μM) as expected since its sequence is derived from the integrin I domain contained in the α subunit of LFA-1, the principal binding site for D1 of ICAM-1. This result agrees with previous findings showing that this peptide inhibits the homotypic T cell adhesion mediated by ICAM-1/LFA-1 interaction [51]. In addition, it indicates that D_1D_2Fc is fully functional in cell-free models and able to bind a peptide derived from LFA-1.

Moreover, our data provide for first time the dissociation constant for ICAM-1 and a peptide agonist. The value obtained (90 nM) is lower than that previously found for the interaction between soluble monomeric ICAM-1 and the high affinity form of its natural ligand LFA-1 (K_d: 500 nM) [59] and higher than that found for dimeric ICAM-1 (K_d: 1-10 nM) [15, 16]. This result provides the biophysical explanation to the capacity of the peptide to block lymphocyte intercellular adhesion as previously reported [51]. In addition, it may help to design novel peptide inhibitors to target this interaction and modulate the immune response [60].

Binding of ICAM-1 chimera to B and T cell-associated LFA-1

ITC experiments indicate that D_1D_2Fc contains the proper folded domains involved in the interaction with a specific sequence derived from integrin I domain of LFA-1α. However, short peptides are lineal aminoacid sequences that do not completely mimic the interaction among proteins containing a three-dimensional spatial structure. Thus, to proves that D_1D_2Fc is active and useful to analyse processes in which ICAM-1/LFA-1 interaction is involved, we have analysed the ability of the purified protein to bind the native form of LFA-1 expressed on the plasma membrane of lymphoid cells. To this aim we tested the ability of immobilised D_1D_2Fc to adhere LFA-1 expressing B cells and the interaction of D_1D_2Fc and LFA-1 in T cells by flow cytometry (Figure 5).

As showed in Figure 5A, D_1D_2Fc is able to mediate the adhesion of activated B lymphocytes showing the highest activity at a concentration of 50 μg/well. Cells incubated with medium alone or in wells coated with IgG1 show extensive clumping and no adherent cells are seen. In contrast, cell clumping is much more reduced in wells coated with D_1D_2Fc and several cells with fibroblast-like morphology can be detected.

The quantification of cell adhesion results in a 10-fold increase related to the negative IgG control.

The activity of this chimera to promote B cell adhesion was lower than that found by using a chimera expressing the 5 domains of ICAM-1 (data not shown). It has been previously reported that D1 presence on a single molecule of ICAM-1 is enough to bind LFA-1 [17] [18]. However, the presence of the 5 domains of ICAM-1 provides a better adhesion as previously suggested [15, 16]. Another explanation could be that the B cells used in this assay expresses Mac-1 that would bind through the D3 domain absent in D_1D_2Fc.

Next, we tested if this chimera was also useful to analyse the expression of LFA-1 in the cell membrane by flow cytometry. To this aim we have used the human T leukemia Jurkat. As shown in Figure 5B the percentage of positive cells increases as it increases the amount of chimera added. The performance of this chimera (1 μg/10^5 cells) to recognise its specific ligand (LFA-1) is similar to that of other chimeras expressed and purified in native form in eukaryotic cells and used to analyse specific ligands in Jurkat cells like NKG2D-Fc (data not shown). Incubation with an antiCD54 (ICAM-1) antibody blocked binding of the chimera (data not shown) showing that D_1D_2Fc is able to specifically bind to Jurkat cells through its natural ligand LFA-1.

As indicated above this result is supported by previous findings indicating that the presence of D_1 is enough to bind LFA-1.

Blocking of NK-cell mediated cytotoxicity

The interaction of ICAM-1, expressed on tumor or virus infected cells, with LFA-1, expressed on the membrane of Natural Killer (NK) cells, modulates the formation and signalling of the NK immunological synapse [61]. This process is critically involved in the elimination of tumor and/or virus-infected cells by NK cells [62]. In order to analyse whether D_1D_2Fc was able to interfere with the cytotoxic function of NK cells, we have tested the ability of this chimera to inhibit the elimination of tumor cells by human NK cells. As can be seen in Figure 6 incubation with increasing amounts of D_1D_2Fc completely blocked cell death induced by human NK wells on the human leukemia K562. Control human IgG1 had no effect on this process (data not shown). Importantly, inhibition was not due to the presence of the Fc region, which is known to bind and activate specific receptors in NK cells, since purified D_1D_2 showed a similar activity. Similar results were found by using the leukemic target cells Raji, Jurkat or U937 (data

not shown). These results indicate that this chimera can also be used to study the processes in which NK cells maybe involved. Moreover, it indicates a good biological activity of the chimera since 100 pg of protein is able to completely block cell death exerted by one NK cell.

Conclusions

To our knowledge, this is the first report on the purification of an active form of ICAM-1 by using a simple and fast bacterial-based method more advantageous than mammalian models, which are very expensive and often difficult to set-up, or than other traditional folding protocols, which are time consuming and require large amounts of reagent such a refolding by dilution. In comparison with refolding by dilution, the most common protocol to purify ICAM-1 in *E. coli* [9], our method shows a reduction in total process time of up to 500% and decreases the cost of up to 150%. If we compare it with mammalian models like HEK or COS cells, the reduction in time and money is much higher. These chimeras are of special interest to study cell adhesion assays, expression of functional ligands on cells by flow cytometry, blocking cell-cell adhesion mediated processes as well as quantification of soluble ligands by ELISA. Our protocol has proven useful in order to analyse several physiological processes in which ICAM-1/LFA-1 interaction is critically involved. Moreover, it is fast and cheap, providing a perfect platform in order to develop large-scale inhibitor screenings or *in vivo* models of ICAM-1 associated pathologies, which are hard to set-up by using commercial purified proteins or other expression systems.

480 **References**

481 **Acknowledgments**

482 This work was supported by grants 2009tw0034 from the Spanish National Research
483 Council (CSIC) and The National Science Council from Taiwan (EMG and AC),
484 SAF2011-25390 from Spanish Ministry of Economy and Competitiveness (JP) and
485 BFU2010-19451 from Spanish Ministry of Science and Innovation (AVC). JP and AVC
486 were supported by Aragón I+D (ARAID). DSM is supported by a fellowship from
487 Gobierno de Aragón. We thank Klaus Ebnet for advice regarding experimental models
488 and ICAM-1 cloning and Adriana Aporta for helping in the establishment of the
489 purification protocol.

490

Table 1. Thermodynamic parameters for the unfolding of D1D2Fc and D1D2 obtained by following the thermal unfolding by intrinsic tryptophan or ANS fluorescence.

	T_{m1} (^oC)	ΔH_1 (kcal/mol)	T_{m2} (^oC)	ΔH_2 (kcal/mol)
D1D2Fc (Trp)	39.1 ± 0.2	20.0 ± 0.3	69 ± 1	51 ± 1
D1D2Fc (ANS)	40.0 ± 0.4	19.5 ± 0.4	70 ± 1	49 ± 1
D1D2 (ANS)	46 ± 1	23 ± 1	65 ± 1	27 ± 1

Figure legends

Figure 1. Schematic representation of the aminoacid sequences of the proteins expressed by using the constructs pET28a-D_1D_2Fc and pET28a-D_1D_2. Numbers indicate the corresponding aminoacids in human ICAM-1 sequence. Histidine tag (H), domain 1 (D_1), domain 2 (D_2), Linker (L), human IgG1 Fc region (Fc).

Figure 2. Analyses of the expression and purification of D_1D_2Fc D_1D_2 in *E. coli* by SDS-PAGE electrophoresis and western blot. Bacteria were transformed by using pET28a-D_1D_2Fc or pET28a-D_1D_2 constructions and proteins were expressed and purified as described in materials and methods. **A** analysis of protein overexpression in bacteria by Coomassie Blue staining after SDS-PAGE. M: MW markers; 1,4: non-induced transformed bacteria; 2, 3, 5, 6: bacteria induced with IPTG for 2h (2 and 5) or 3h (3 and 6). **B and D**, analysis of protein refolding and purification by Coomassie Blue staining after SDS-PAGE. M: MW markers; 1: induction with IPTG; 2-4 non-bound proteins; 5-6: folding steps; 7-15: elution with Imidazole. **C and E**, purified proteins were separated by SDS-PAGE and analysed by western blot using antibodies specific against ICAM-1 (lane 1) or poly-histidine tag (lane 2).

Figure 3. Spectroscopic structural characterization. **A**, Circular Dichroism spectra of D_1D_2Fc recorded in the far ultraviolet region (200nm-250nm). **B**, Thermal denaturation. i) Tryptophan fluorescence emission spectra of D_1D_2Fc (protein 2 μM in PBS buffer). Inset: Tryptophan fluorescence emission spectra of D_1D_2 under the same conditions; ii), Thermal unfolding of D_1D_2Fc followed by tryptophan intrinsic fluorescence emission at 330 nm. The temperature dependence of the fluorescence intensity at 330 nm was fitted to a 2-transition unfolding model; iii) ANS fluorescence emission spectra of D_1D_2Fc (protein 2 μM and ANS 100 μM in PBS buffer); iv) Thermal unfolding of D_1D_2Fc followed by ANS fluorescence. The temperature dependence of the fluorescence average energy of the ANS spectrum was fitted to a 2-transition unfolding model. A similar result was obtained when the temperature dependence of the ANS fluorescence emission at 470 nm was fitted to a 2-transition unfolding model; v) ANS fluorescence emission spectra of D_1D_2. Protein 2 μM and ANS 100 μM in PBS buffer; vi) Thermal unfolding of D_1D_2 followed by ANS fluorescence. The temperature dependence of the fluorescence average energy of the ANS spectrum was fitted to a 2-transition unfolding model. A similar result was obtained when the temperature dependence of the ANS fluorescence emission at 470 nm was fitted to a 2-transition unfolding model.

Figure 4. Interaction of LFA-1 peptide with D_1D_2Fc by isothermal titration calorimetry (ITC). Purified D_1D_2Fc (12 μM) was titrated with a peptide derived from the binding site of LFA-1 (150 μM). The assay was performed in PBS buffer at 25°C. The non-linear regression analysis provided a dissociation constant of 91 nM.

Figure 5. Binding of D_1D_2Fc to cell-associated LFA-1. **A**, B cell adhesion assay. Different amounts of D_1D_2Fc or human IgG1 control were immobilised in 96 well plates o.n. at 4ºC. After washing out non-bound protein, the PMA-activated R69 B cell line was added by triplicates and cell adhesion was analysed by MTT as described in materials and methods. Quantification of cell binding was represented as fold increase with respect to the human IgG1 control. **B**, analysis of D_1D_2Fc binding to LFA-1 in Jurkat cells by flow cytometry. Different amounts of D_1D_2Fc or human IgG1 control were incubated with Jurkat cells. After washing out non non-bound proteins cells were incubated with PE-conjugated goat anti-human IgG Fcγ Ab and analysed by flow cytometry. A representative histogram is shown. Numbers correspond to the % of cells as gated by the vertical bars. Black: goat anti-human IgG; Grey: human IgG1; Colour: D_1D_2Fc (red: 5 μg; green: 10 μg; blue: 15 μg). Values in the graph are represented as mean+/- SEM of 3 independent experiments performed by duplicate. Statistical analyses were done with two-way ANOVA with Bonferroni post-test by comparing IgG with D_1D_2Fc. ns: not statistically significant; *** $p<0.001$.

Figure 6. D_1D_2Fc inhibits NK-cell mediated cytotoxicity on tumor cells. MACS-enriched human NK cells, previously stained with the fluorescence dye CFSE, were incubated with K562 cells at 1:1 effector:target ratio ($1x10^5$ cells) for 4h in the presence or absence of different amounts of D_1D_2Fc, D_1D_2 or human IgG1 control. Subsequently, cell death was analysed by measuring PS translocation by flow cytometry in the CFSE negative cell population (K562) as described in materials and methods. Values are represented as mean+/- SEM of 2 different experiments. Statistical analyses were done with two-way ANOVA with Bonferroni post-test by comparing IgG, D_1D_2 and D_1D_2Fc with control. ns: not statistically significant; *** $p<0.001$.

[1] Springer TA. Adhesion receptors of the immune system. Nature 1990;346:425-434.

[2] Lawson C, Wolf S. ICAM-1 signaling in endothelial cells. Pharmacol Rep 2009;61:22-32.

[3] Long EO. ICAM-1: getting a grip on leukocyte adhesion. J Immunol 2011;186:5021-5023.

[4] Fuchs R, Blaas D. Uncoating of human rhinoviruses. Rev Med Virol 2010;20:281-297.

[5] Berendt AR, McDowall A, Craig AG, Bates PA, Sternberg MJ, Marsh K, Newbold CI, Hogg N. The binding site on ICAM-1 for Plasmodium falciparum-infected erythrocytes overlaps, but is distinct from, the LFA-1-binding site. Cell 1992;68:71-81.

[6] Ockenhouse CF, Betageri R, Springer TA, Staunton DE. Plasmodium falciparum-infected erythrocytes bind ICAM-1 at a site distinct from LFA-1, Mac-1, and human rhinovirus. Cell 1992;68:63-69.

[7] Bernabeu M, Lopez FJ, Ferrer M, Martin-Jaular L, Razaname A, Corradin G, Maier AG, Del Portillo HA, Fernandez-Becerra C. Functional analysis of Plasmodium vivax VIR proteins reveals different subcellular localizations and cytoadherence to the ICAM-1 endothelial receptor. Cell Microbiol 2012;14:386-400.

[8] Diamond MS, Staunton DE, Marlin SD, Springer TA. Binding of the integrin Mac-1 (CD11b/CD18) to the third immunoglobulin-like domain of ICAM-1 (CD54) and its regulation by glycosylation. Cell 1991;65:961-971.

[9] Martin S, Martin A, Staunton DE, Springer TA. Functional studies of truncated soluble intercellular adhesion molecule 1 expressed in Escherichia coli. Antimicrob Agents Chemother 1993;37:1278-1284.

[10] Staunton DE, Dustin ML, Erickson HP, Springer TA. The arrangement of the immunoglobulin-like domains of ICAM-1 and the binding sites for LFA-1 and rhinovirus. Cell 1990;61:243-254.

[11] Landis RC, McDowall A, Holness CL, Littler AJ, Simmons DL, Hogg N. Involvement of the "I" domain of LFA-1 in selective binding to ligands ICAM-1 and ICAM-3. J Cell Biol 1994;126:529-537.

[12] Huang C, Springer TA. A binding interface on the I domain of lymphocyte function-associated antigen-1 (LFA-1) required for specific interaction with intercellular adhesion molecule 1 (ICAM-1). J Biol Chem 1995;270:19008-19016.

[13] Staunton DE, Merluzzi VJ, Rothlein R, Barton R, Marlin SD, Springer TA. A cell adhesion molecule, ICAM-1, is the major surface receptor for rhinoviruses. Cell 1989;56:849-853.

[14] Duperray A, Languino LR, Plescia J, McDowall A, Hogg N, Craig AG, Berendt AR, Altieri DC. Molecular identification of a novel fibrinogen binding site on the first domain of ICAM-1 regulating leukocyte-endothelium bridging. J Biol Chem 1997;272:435-441.

[15] Miller J, Knorr R, Ferrone M, Houdei R, Carron CP, Dustin ML. Intercellular adhesion molecule-1 dimerization and its consequences for adhesion mediated by lymphocyte function associated-1. J Exp Med 1995;182:1231-1241.

[16] Reilly PL, Woska JR, Jr., Jeanfavre DD, McNally E, Rothlein R, Bormann BJ. The native structure of intercellular adhesion molecule-1 (ICAM-1) is a dimer. Correlation with binding to LFA-1. J Immunol 1995;155:529-532.

[17] Casasnovas JM, Stehle T, Liu JH, Wang JH, Springer TA. A dimeric crystal structure for the N-terminal two domains of intercellular adhesion molecule-1. Proc Natl Acad Sci U S A 1998;95:4134-4139.

[18] Jun CD, Shimaoka M, Carman CV, Takagi J, Springer TA. Dimerization and the effectiveness of ICAM-1 in mediating LFA-1-dependent adhesion. Proc Natl Acad Sci U S A 2001;98:6830-6835.

[19] Martin S, Heidenthal E, Schulte B, Rothe H, Kolb H. Soluble forms of intercellular adhesion molecule-1 inhibit insulitis and onset of autoimmune diabetes. Diabetologia 1998;41:1298-1303.

[20] Oh HM, Kwon MS, Kim HJ, Jeon BH, Kim HR, Choi HO, Na BR, Eom SH, Song NW, Jun CD. Intermediate monomer-dimer equilibrium structure of native ICAM-1: implication for enhanced cell adhesion. Exp Cell Res 2011;317:163-172.

[21] Springer TA. Traffic signals for lymphocyte recirculation and leukocyte emigration: the multistep paradigm. Cell 1994;76:301-314.

[22] Millan J, Hewlett L, Glyn M, Toomre D, Clark P, Ridley AJ. Lymphocyte transcellular migration occurs through recruitment of endothelial ICAM-1 to caveola- and F-actin-rich domains. Nat Cell Biol 2006;8:113-123.

[23] Springer TA, Dustin ML. Integrin inside-out signaling and the immunological synapse. Curr Opin Cell Biol 2012;24:107-115.

[24] Frank PG, Lisanti MP. ICAM-1: role in inflammation and in the regulation of vascular permeability. Am J Physiol Heart Circ Physiol 2008;295:H926-H927.

[25] Kobayashi H, Boelte KC, Lin PC. Endothelial cell adhesion molecules and cancer progression. Curr Med Chem 2007;14:377-386.

[26] Rosette C, Roth RB, Oeth P, Braun A, Kammerer S, Ekblom J, Denissenko MF. Role of ICAM1 in invasion of human breast cancer cells. Carcinogenesis 2005;26:943-950.

[27] Miele ME, Bennett CF, Miller BE, Welch DR. Enhanced metastatic ability of TNF-alpha-treated malignant melanoma cells is reduced by intercellular adhesion molecule-1 (ICAM-1, CD54) antisense oligonucleotides. Exp Cell Res 1994;214:231-241.

[28] Zheng Y, Yang J, Qian J, Qiu P, Hanabuchi S, Lu Y, Wang Z, Liu Z, Li H, He J, Lin P, Weber D, Davis RE, Kwak L, Cai Z, Yi Q. PSGL-1/selectin and ICAM-1/CD18 interactions are involved in macrophage-induced drug resistance in myeloma. Leukemia 2012.

[29] Iigo Y, Takashi T, Tamatani T, Miyasaka M, Higashida T, Yagita H, Okumura K, Tsukada W. ICAM-1-dependent pathway is critically involved in the pathogenesis of adjuvant arthritis in rats. J Immunol 1991;147:4167-4171.

[30] Galkina E, Ley K. Vascular adhesion molecules in atherosclerosis. Arterioscler Thromb Vasc Biol 2007;27:2292-2301.

[31] Eksteen B, Liaskou E, Adams DH. Lymphocyte homing and its role in the pathogenesis of IBD. Inflamm Bowel Dis 2008;14:1298-1312.

[32] Thomas S, Baumgart DC. Targeting leukocyte migration and adhesion in Crohn's disease and ulcerative colitis. Inflammopharmacology 2012;20:1-18.

[33] Huang WC, Chan ST, Yang TL, Tzeng CC, Chen CC. Inhibition of ICAM-1 gene expression, monocyte adhesion and cancer cell invasion by targeting IKK complex: molecular and functional study of novel alpha-methylene-gamma-butyrolactone derivatives. Carcinogenesis 2004;25:1925-1934.

[34] Shimaoka M, Springer TA. Therapeutic antagonists and the conformational regulation of the beta2 integrins. Curr Top Med Chem 2004;4:1485-1495.

[35] Anderson ME, Siahaan TJ. Targeting ICAM-1/LFA-1 interaction for controlling autoimmune diseases: designing peptide and small molecule inhibitors. Peptides 2003;24:487-501.

[36] Porath J, Carlsson J, Olsson I, Belfrage G. Metal chelate affinity chromatography, a new approach to protein fractionation. Nature 1975;258:598-599.

[37] Hutchens TW, Yip TT. Protein interactions with immobilized transition metal ions: quantitative evaluations of variations in affinity and binding capacity. Anal Biochem 1990;191:160-168.

[38] Lilie H, Schwarz E, Rudolph R. Advances in refolding of proteins produced in E. coli. Curr Opin Biotechnol 1998;9:497-501.

[39] Zardeneta G, Horowitz PM. Protein refolding at high concentrations using detergent/phospholipid mixtures. Anal Biochem 1994;218:392-398.

[40] Gu Z, Weidenhaupt M, Ivanova N, Pavlov M, Xu B, Su ZG, Janson JC. Chromatographic methods for the isolation of, and refolding of proteins from, Escherichia coli inclusion bodies. Protein Expr Purif 2002;25:174-179.

[41] Shalongo W, Ledger R, Jagannadham MV, Stellwagen E. Refolding of denatured thioredoxin observed by size-exclusion chromatography. Biochemistry 1987;26:3135-3141.

[42] Fahey EM, Chaudhuri JB, Binding P. Refolding and purification of a urokinase plasminogen activator fragment by chromatography. J Chromatogr B Biomed Sci Appl 2000;737:225-235.

[43] Schlegl R, Iberer G, Machold C, Necina R, Jungbauer A. Continuous matrix-assisted refolding of proteins. J Chromatogr A 2003;1009:119-132.

[44] Geng X, Bai Q, Zhang Y, Li X, Wu D. Refolding and purification of interferon-gamma in industry by hydrophobic interaction chromatography. J Biotechnol 2004;113:137-149.

[45] Stempfer G, Holl-Neugebauer B, Rudolph R. Improved refolding of an immobilized fusion protein. Nat Biotechnol 1996;14:329-334.

[46] Umakoshi H, Persson J, Kroon M, Johansson HO, Otzen DE, Kuboi R, Tjerneld F. Model process for separation based on unfolding and refolding of chymotrypsin inhibitor 2 in thermoseparating polymer two-phase systems. J Chromatogr B Biomed Sci Appl 2000;743:13-19.

[47] Oganesyan N, Kim SH, Kim R. On-column protein refolding for crystallization. J Struct Funct Genomics 2005;6:177-182.

[48] Rogl H, Kosemund K, Kuhlbrandt W, Collinson I. Refolding of Escherichia coli produced membrane protein inclusion bodies immobilised by nickel chelating chromatography. FEBS Lett 1998;432:21-26.

[49] Colangeli R, Heijbel A, Williams AM, Manca C, Chan J, Lyashchenko K, Gennaro ML. Three-step purification of lipopolysaccharide-free, polyhistidine-tagged recombinant antigens of Mycobacterium tuberculosis. J Chromatogr B Biomed Sci Appl 1998;714:223-235.

[50] Lemercier C, Legube G, Caron C, Louwagie M, Garin J, Trouche D, Khochbin S. Tip60 acetyltransferase activity is controlled by phosphorylation. J Biol Chem 2003;278:4713-4718.

[51] Tibbetts SA, Seetharama Jois D, Siahaan TJ, Benedict SH, Chan MA. Linear and cyclic LFA-1 and ICAM-1 peptides inhibit T cell adhesion and function. Peptides 2000;21:1161-1167.

[52] Paradela A, Garcia-Peydro M, Vazquez J, Rognan D, Lopez de Castro JA. The same natural ligand is involved in allorecognition of multiple HLA-B27 subtypes by a single T cell clone: role of peptide and the MHC molecule in alloreactivity. J Immunol 1998;161:5481-5490.

[53] Rothlein R, Dustin ML, Marlin SD, Springer TA. A human intercellular adhesion molecule (ICAM-1) distinct from LFA-1. J Immunol 1986;137:1270-1274.

[54] Alley MC, Scudiero DA, Monks A, Hursey ML, Czerwinski MJ, Fine DL, Abbott BJ, Mayo JG, Shoemaker RH, Boyd MR. Feasibility of drug screening with panels of human tumor cell lines using a microculture tetrazolium assay. Cancer Res 1988;48:589-601.

[55] Bernardo I, Mancebo E, Aguilo I, Anel A, Allende LM, Guerra-Vales JM, Ruiz-Contreras J, Serrano A, Talayero P, de la Calle O, Gonzalez-Santesteban C, Paz-Artal E. Phenotypic and functional evaluation of CD3+CD4-CD8- T cells in human CD8 immunodeficiency. Haematologica 2011;96:1195-1203.

[56] Pardo J, Galvez EM, Koskinen A, Simon MM, Lobigs M, Regner M, Mullbacher A. Caspase-dependent inhibition of mousepox replication by gzmB. PLoS One 2009;4:e7512.

[57] Glynou K, Ioannou PC, Christopoulos TK. One-step purification and refolding of recombinant photoprotein aequorin by immobilized metal-ion affinity chromatography. Protein Expr Purif 2003;27:384-390.

[58] Staunton DE, Marlin SD, Stratowa C, Dustin ML, Springer TA. Primary structure of ICAM-1 demonstrates interaction between members of the immunoglobulin and integrin supergene families. Cell 1988;52:925-933.

[59] Tominaga Y, Kita Y, Satoh A, Asai S, Kato K, Ishikawa K, Horiuchi T, Takashi T. Affinity and kinetic analysis of the molecular interaction of ICAM-1 and leukocyte function-associated antigen-1. J Immunol 1998;161:4016-4022.

[60] Zhou CL, Lu R, Lin G, Yao Z. The latest developments in synthetic peptides with immunoregulatory activities. Peptides 2011;32:408-414.

[61] Liu D, Bryceson YT, Meckel T, Vasiliver-Shamis G, Dustin ML, Long EO. Integrin-dependent organization and bidirectional vesicular traffic at cytotoxic immune synapses. Immunity 2009;31:99-109.

[62] Bryceson YT, March ME, Barber DF, Ljunggren HG, Long EO. Cytolytic granule polarization and degranulation controlled by different receptors in resting NK cells. J Exp Med 2005;202:1001-1012.

- we have established a fast and cost-effective method to produce recombinant human ICAM-1
- ICAM-1 presents a proper folding as revealed by analyses of secondary and tertiary structure
- purified ICAM-1 is highly active and proves useful for biochemical, immunological and cell biology studies.
- ICAM-1 has been used to calculate the dissociation constant of peptide inhibitors used to treat inflammatory disorders

Figure 1.jpg

Figure 1

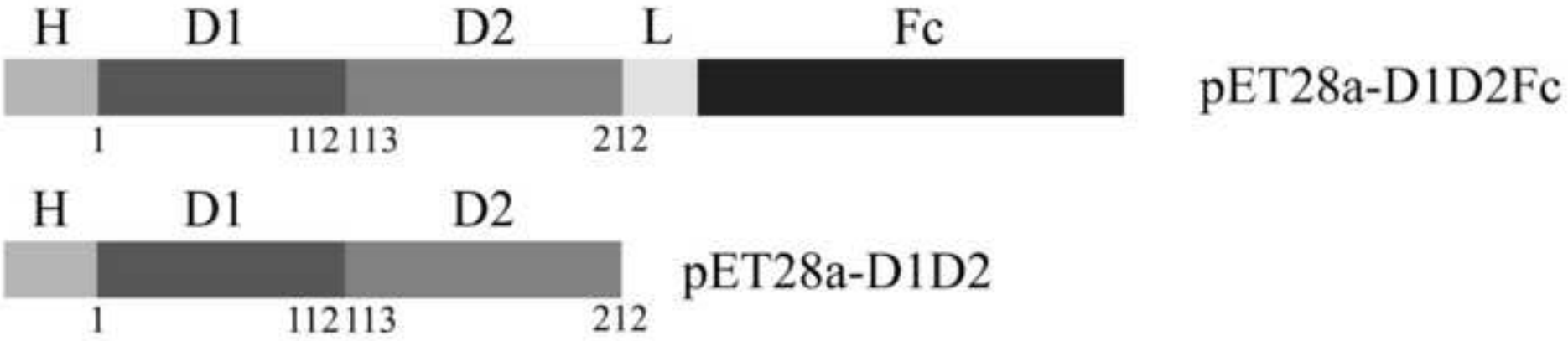

Figure 2.jpg

Figure 2

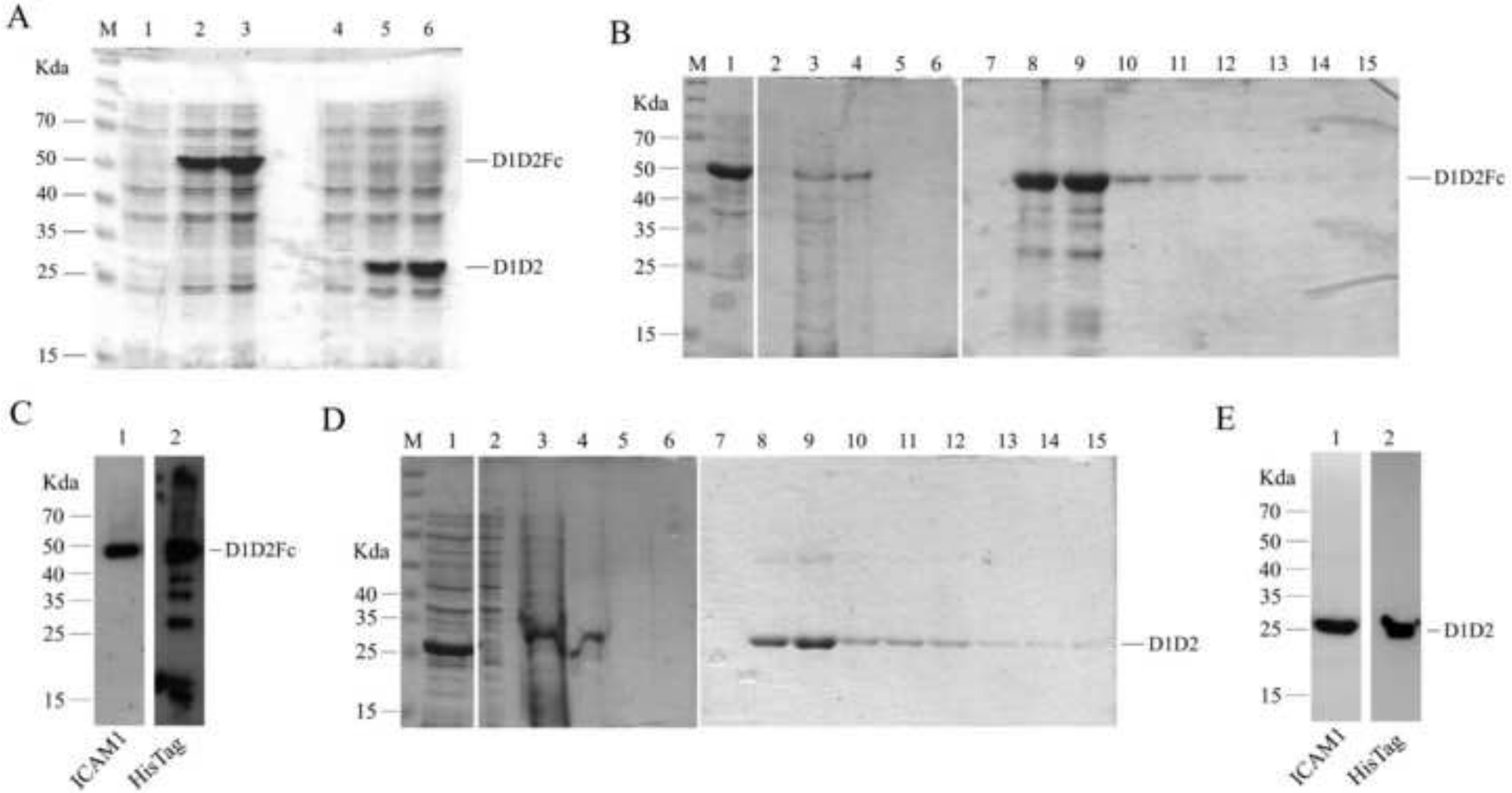

Figure 3

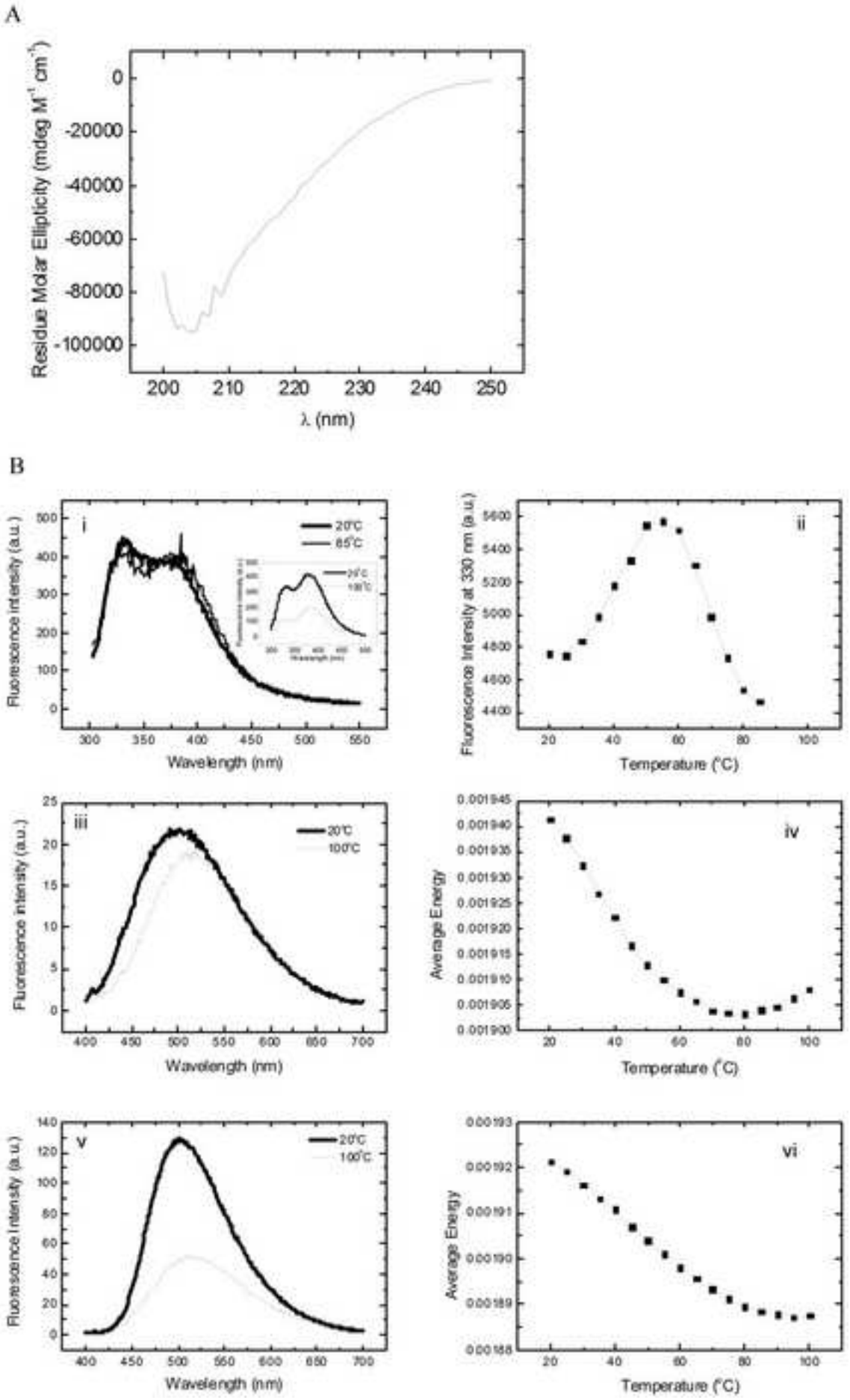

Figure 4

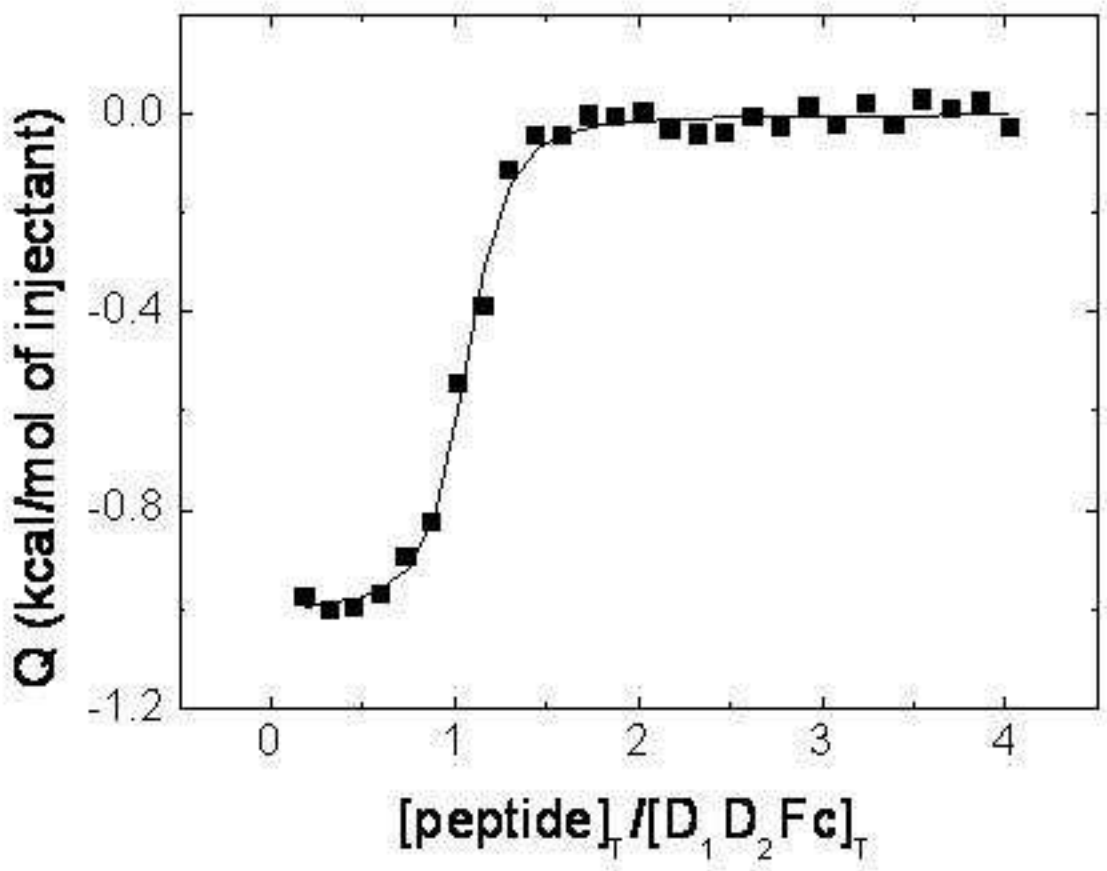

Figure 5

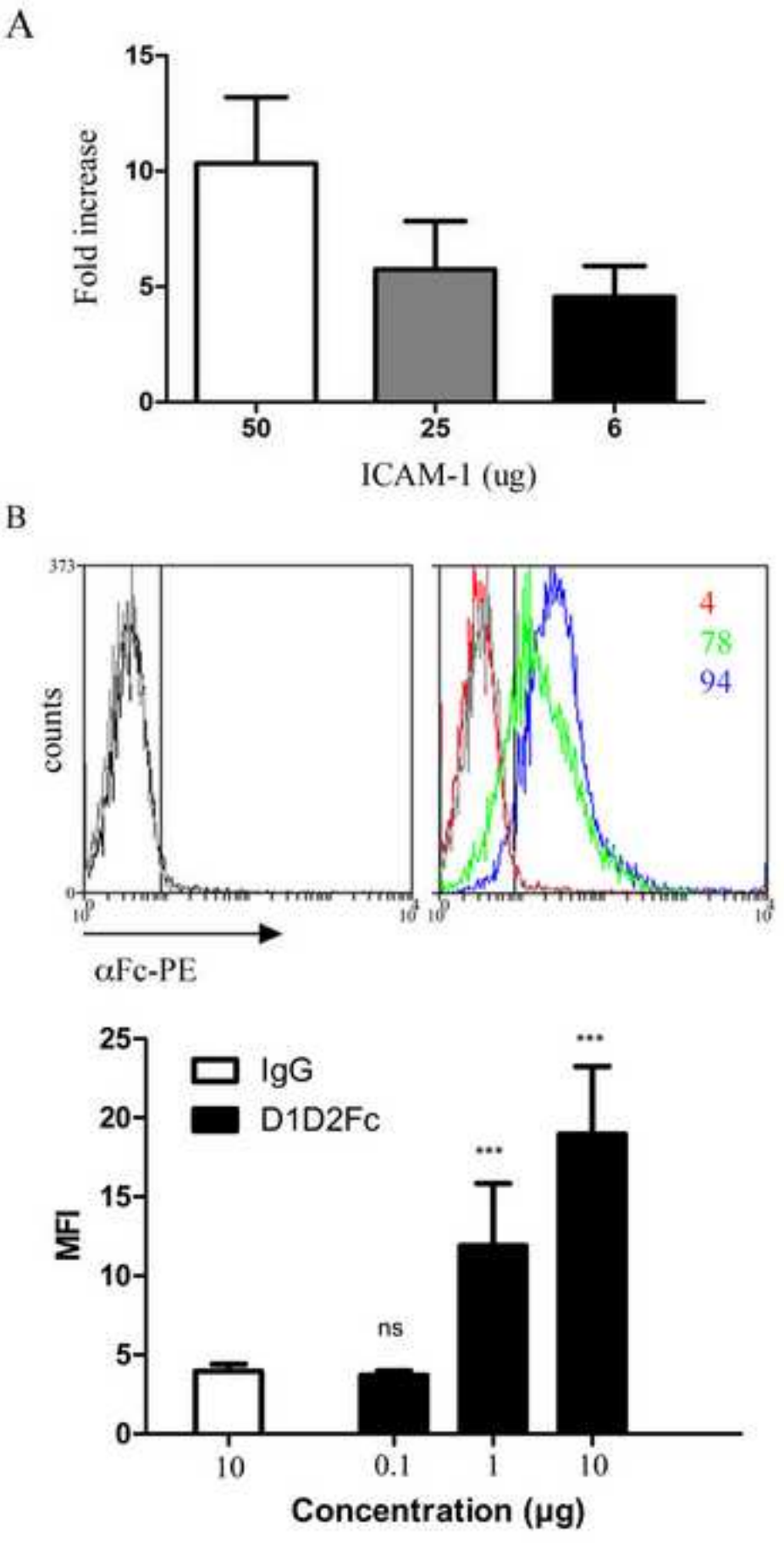

Figure 6.jpg

Figure 6